

Fig. 3. System construction of sensing node.

Table 1. Specification of node control board.

CPU	32bit RISC processor
Clock	200MHz
Memory :	Flash 4MB, SDRAM 32MB, cash SRAM 16kB
Port	8bit DIO 8ports, Serial 3 ports (IrDA, USB,...)
Voltage	3.3[V]
Power	0.683 [W]
[AD Converter]	Input : 8 channels (0 – 3.6V) Resolution : 10bit Conversion time : 16 [micro sec]
[DA Converter]	Output : 2 channels (0 – 3.6V) Resolution : 8bit Conversion time : 10 [micro sec]

Table 2. Specification of wireless communication unit.

Band frequency	1216 MHz
Baud Rate	9800 bps
Voltage	3V
Power	0.18W

Table 3. Specification of GPS unit.

Receive	12 parallel ch
Acquisition Time	15 – 45 sec.
Update Time	1 sec.
Position Accuracy	1 – 5 m
Information	North latitude, East longitude Absolute Time (hh/mm/ss)
Voltage	3 V

2. ACCELERATION SIGNAL MEASURING IN SENSING NODE

At no acceleration to sensing node, output signal of acceleration sensor becomes a constant voltage (normal mode). When the acceleration to sensing node by landslide or collision with hard blocks occurs, the signal fluctuates on the constant voltage level. To investigate the characteristics of acceleration in these situations of sensing node, we have observed the acceleration signals.

Fig. 4 shows an acceleration signal $x_{col}(t)$ occurred by the collision between a sensing node and a weight(120g) for

0.9sec.. The weight was fallen down from 1 m height on the sensing node. The acceleration signal was composed with signals of three directions(X, Y, Z).

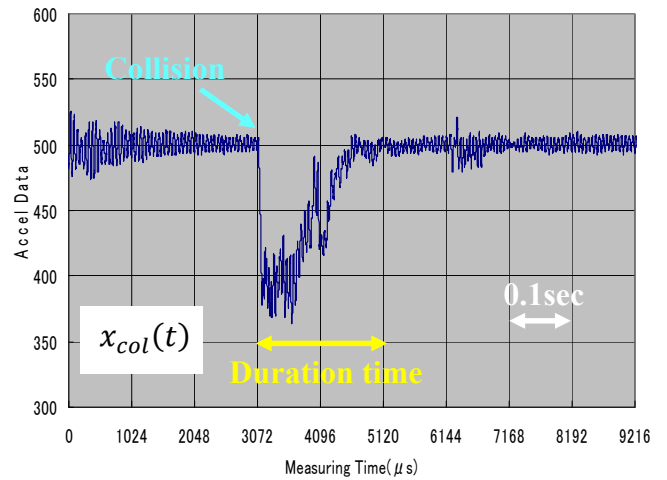


Fig. 4. Acceleration signal by the collision between a sensing node and a weight(120g).

In Fig.4, the acceleration signal $x_{col}(t)$ is single phenomenon. The waveform of signal $x_{col}(t)$ is isolate. The duration time is 0.2 sec approximately. The duration time is depended on the quantity of weight. In case that heavy weight hits the sensing node, the amplitude of signal $x_{col}(t)$ becomes higher and the duration time becomes longer a little.

Fig. 5 shows an acceleration signal $x_{slid}(t)$ from the sensing node sliding down on slope for 0.9sec. indoor. Angle of the slope is 35 degree. In this case, the sensing node was not rolling itself.

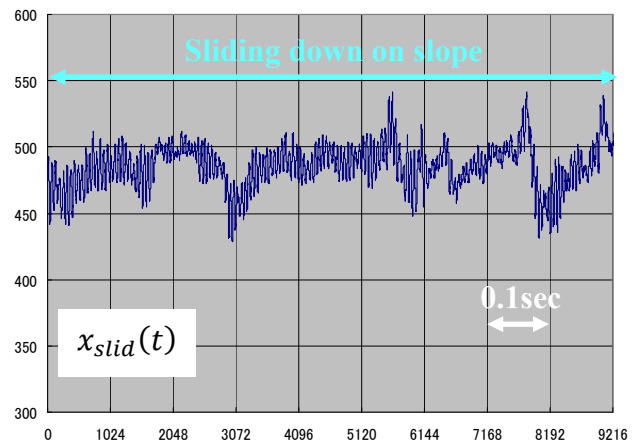


Fig. 5. Acceleration signal from the sensing node sliding down on slope.

In Fig.5, the acceleration signal $x_{slid}(t)$ fluctuates continuously. The amplitude is not so high, but the voltage level distinguished with noise signal on a constant voltage. The waveform of signal $x_{slid}(t)$ is depended on speed of sliding. When the sensing node slides on slop quickly, the amplitude of signal $x_{slid}(t)$ becomes lower a little.

Fig. 6 shows an acceleration signal $x_{roll}(t)$ from the sensing node rolling down on slope for 0.9sec. indoor. Angle of the slope is 35 degree. In rolling down, the sensing node had been jumping and hitting on slope

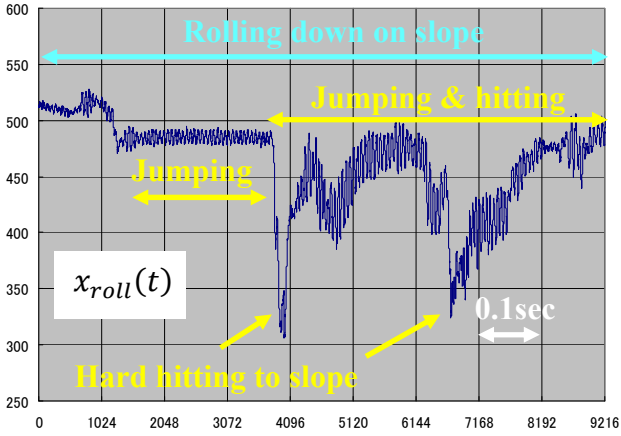


Fig. 6. Acceleration signal from the sensing node rolling down on slope.

In Fig. 6, the waveform of acceleration signal $x_{roll}(t)$ became complex fluctuation. In the time that sensing node was big jumping, the acceleration signal $x_{roll}(t)$ became constant. At the time that the sensing node was hitting to slope, the acceleration signal $x_{roll}(t)$ had high amplitude in a moment. Generally, the sensing node repeated small jumps and hits on slope.

3. TIME TRANSITION OF FREQUENCY DISTRIBUTIONS OF ACCELERATION SIGNAL

On consideration by observing these signals $x_{col}(t)$, $x_{slid}(t)$, $x_{roll}(t)$, it is impossible to distinguish landslide by only comparing with a constant threshold level and the amplitude of signals $x_{col}(t)$, $x_{slid}(t)$, $x_{roll}(t)$. Then, to observe the characteristics of acceleration signal $x(t)$ in frequency domain, we have calculated frequency distribution $X(n)$ ($n = 1, 2, 3, \dots$) of that signal $x(t)$ each time interval. The frequency distribution $X(n)$ is generated by the Fast Fourier Transformation (FFT) of 1024 sample data in a time interval (approximately 0.1 sec). To investigate the changing of acceleration signal $x(t)$ each time interval, it is so useful to monitor the time transition of frequency distributions (TTFDs). Following sections show the TTFDs in cases of three kinds of situation of the sensing node.

3.1. TTFDs in case of collision with sensing node and a weight

Fig.7 shows the acceleration signal $x_{col}(t)$ and the TTFDs ($X_{col,4}(n)$, $X_{col,5}(n)$, $X_{col,6}(n)$, $X_{col,7}(n)$) by the collision with the sensing node and a weight (120g). Each frequency distribution covers the 1st - 20th order harmonics ($n = 1, 2, 3, \dots, 20$). The frequency resolution is 10Hz.

In the TTFDs, the 1st - 15th order harmonics in $X_{col,4}(n)$ and $X_{col,5}(n)$ disappear in $X_{col,6}(n)$ and $X_{col,7}(n)$. Because

the duration time by collision exists in $x_{col,4}(t)$ and $x_{col,5}(t)$. This difference is so conspicuous at $X_{col}(1), X_{col}(2), X_{col}(3)$.

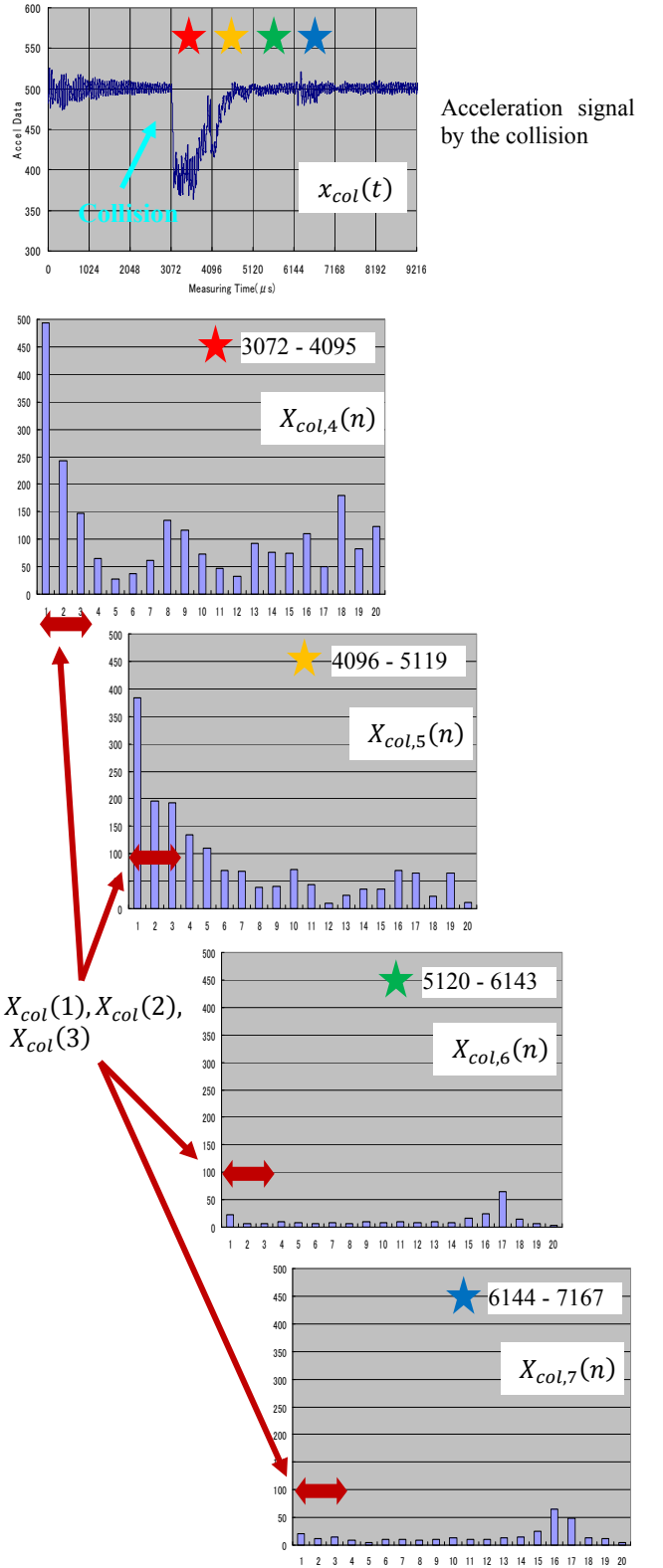
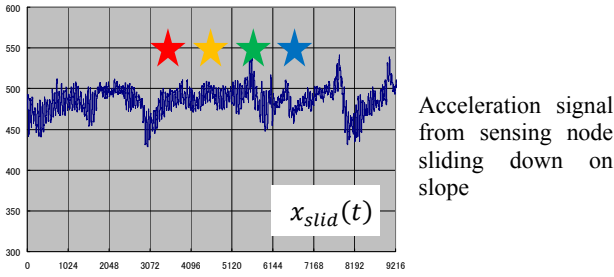


Fig. 7. Time transition of frequency distributions of acceleration signal by the collision with the sensing node and a weight(120g).



Acceleration signal from sensing node sliding down on slope

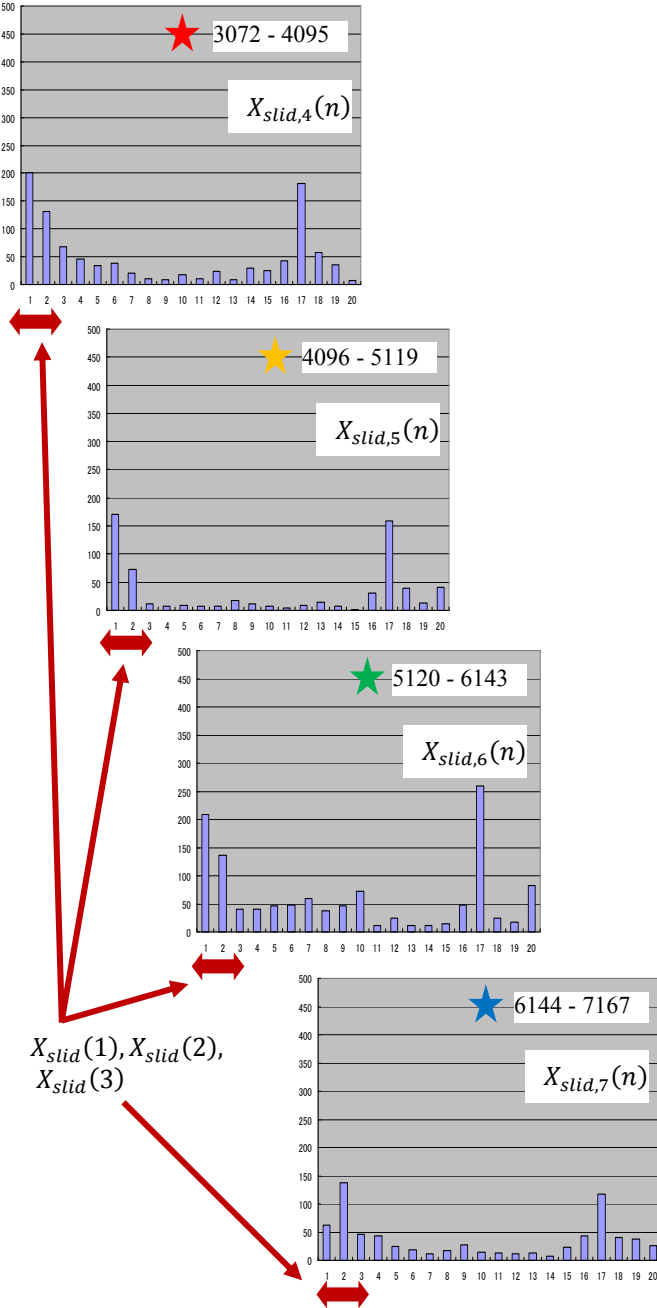


Fig. 8. Time transition of frequency distribution of acceleration signal from the sensing node sliding down on slope.

3.2. TTFDs in case that sensing node is sliding down on slope

Fig. 8 shows the acceleration signal $x_{slid}(t)$ and the TTFDs ($X_{slid,4}(n)$, $X_{slid,5}(n)$, $X_{slid,6}(n)$, $X_{slid,7}(n)$) from the sensing node sliding down on slope.

In the TTFDs, the 1st and 2nd order harmonics $X_{col}(1)$ and $X_{col}(2)$ appear constantly. Other harmonics appear randomly.

3.3. TTFDs in case that sensing node is rolling down on slope

Fig. 9 shows the acceleration signal $x_{roll}(t)$ and the TTFDs ($X_{roll,4}(n)$, $X_{roll,5}(n)$, $X_{roll,6}(n)$, $X_{roll,7}(n)$) from the sensing node rolling down on slope.

$X_{roll,4}(n)$ and $X_{roll,7}(n)$ are the frequency distributions at temporal collisions between the rolling sensing node and slope. In the TTFDs, the 1st - 3rd order harmonics of them become high conspicuously. The $X_{roll,5}(n)$ and $X_{roll,6}(n)$ are the frequency distributions at jumping of sensing node. In the TTFDs, the 1st - 4th order harmonics of them resemble the harmonics ($X_{slid}(1)$, $X_{slid}(2)$, $X_{slid}(3)$, $X_{slid}(4)$) of the frequency distribution at sliding down.

As the sensing node repeats jumping and collision at rolling down on slope, the situation of the 1st - 3rd order harmonics of the frequency distribution also repeat. But that the repeats of jumping and collision are not periodically, it is like random.

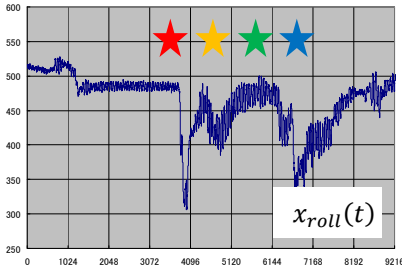
4. DISCUSSIONS OF DISTINCTION OF LANDSLIDE

By observing these acceleration signals $x_{col}(t)$, $x_{slid}(t)$, $x_{roll}(t)$ and the TTFDs of $X_{col}(n)$, $X_{slid}(n)$, $X_{roll}(n)$, it has become obvious that the dynamic behaviours of the 1st - 3rd order harmonics of frequency distribution are characteristic each signal. This means that the distinction of landslide is possible by using only the acceleration information of sensing node.

By the dynamic characteristic of the 1st - 3rd order harmonics of frequency distribution, at following sections, the distinction of collision to sensing node, and the distinction of situation (sliding/rolling down) of sensing node in landslide are discussed. Additionally, for the distinction, some models of the condition based on the situations of their harmonics are proposed. By using these conditions, the sensing node will distinguish the collision and landslide autonomously.

4.1. Distinction of the collision to sensing node

The acceleration signal $x_{col}(t)$ is isolated. In the TTFDs, the intensity of $X_{col}(1)$, $X_{col}(2)$, $X_{col}(3)$ become high only in a short time. Then, if the influence expressed on the 1st - 3rd order harmonics $X(1)$, $X(2)$, $X(3)$ of frequency distribution disappears within a certain time T_1 , it is considered that the responses are caused by the collision to sensing node with a hard block. The time T_1 is defined by the intensity of collision. It will be got by several experiments.



Acceleration signal from sensing node rolling down on slope

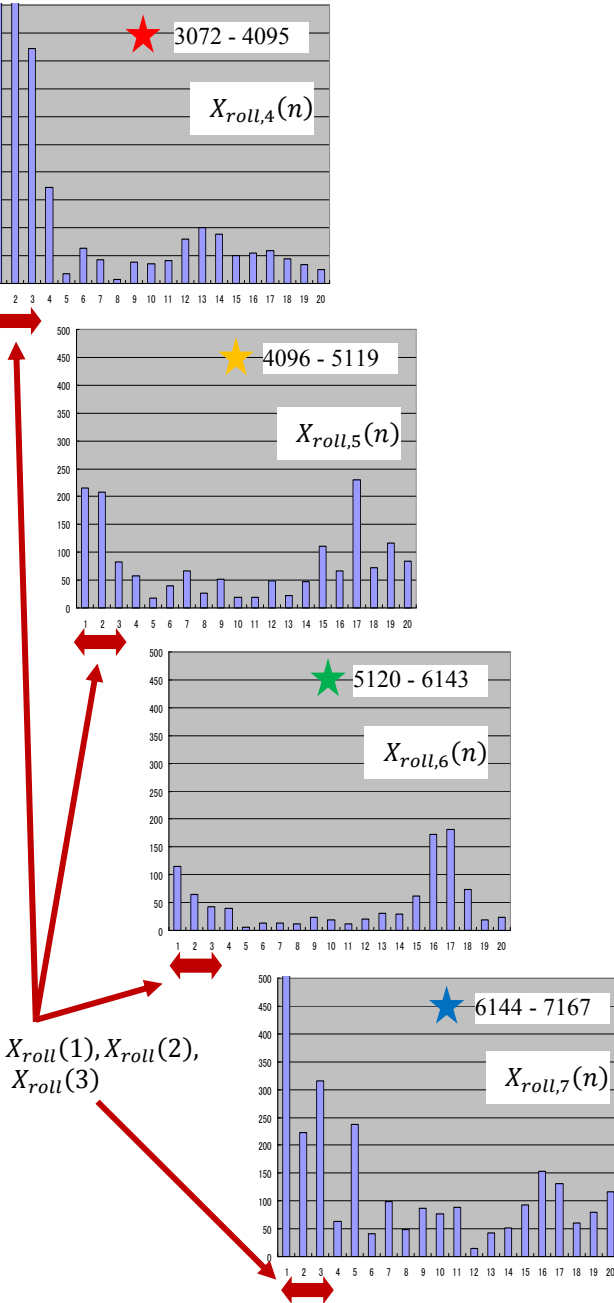


Fig. 9. Time transition of frequency distribution of acceleration signal from the sensing node rolling down on slope.

By using the sum of $X(1)$, $X(2)$, $X(3)$ and a threshold level α , the condition of distinction for the collision is defined as follows,

[Condition_1]

$$\begin{aligned}
 & \text{if } \left(\sum_{n=1}^3 X_k(n) > \alpha \right) \\
 & \quad \{ \text{if } \{ \\
 & \quad \quad \left(\sum_{n=1}^3 X_{k+2}(n) < \alpha \right) \\
 & \quad \quad \cap \left(\sum_{n=1}^3 X_{k+3}(n) < \alpha \right) \\
 & \quad \quad \quad \vdots \\
 & \quad \quad \cap \left(\sum_{n=1}^3 X_{k+9}(n) < \alpha \right) \\
 & \quad \quad \} \\
 & \quad \text{then } \{ \\
 & \quad \quad [\text{the occurrence of collision, not landslide}] \\
 & \quad \quad \} \\
 & \quad \} \\
 & \text{where } T_1 = 1 \text{ sec. (10 segments : } k, k+1, \dots, k+9).
 \end{aligned}$$

The threshold level α and the time T_1 will be defined by several experiments.

4.2. Distinction of the landslide sensed by sliding down of sensing node

The acceleration signal $x_{slid}(t)$ fluctuates continuously. In the TTFDs, the 1st and 2nd order harmonics $X_{slid}(1)$ and $X_{slid}(2)$ appear constantly in sliding down of sensing node. Then, if the influence expressed on the 1st - 2nd order harmonics $X(1)$, $X(2)$ of frequency distribution appear continuously over a certain time T_2 , it is considered that the responses are caused by the sliding down of sensing node in landslide. The time T_2 is longer time than the time T_1 defined by the intensity of collision. It will be got by several experiments.

By using the sum of $X(1)$, $X(2)$ and threshold levels β and γ ($\gamma > \beta$), the condition of distinction for the landslide sensed by sliding down of sensing node is defined as follows,

[Condition_2]

$$\begin{aligned}
 & \text{if } \left(\gamma > \sum_{n=1}^2 X_k(n) > \beta \right) \\
 & \quad \{ \text{if } \{ \\
 & \quad \quad \left(\gamma > \sum_{n=1}^2 X_{k+2}(n) > \beta \right) \\
 & \quad \quad \cap \left(\gamma > \sum_{n=1}^2 X_{k+3}(n) > \beta \right) \\
 & \quad \quad \quad \vdots \\
 & \quad \quad \cap \left(\gamma > \sum_{n=1}^2 X_{k+9}(n) > \beta \right) \\
 & \quad \quad \} \\
 & \quad \text{then } \{ \\
 & \quad \quad [\text{the occurrence of landslide}] \\
 & \quad \quad \} \\
 & \quad \} \\
 & \text{where } T_2 = 1 \text{ sec. (10 segments : } k, k+1, \dots, k+9).
 \end{aligned}$$

The threshold levels β , γ and the time T_2 will be defined by several experiments.

4.3. Distinction of the landslide sensed by rolling down of sensing node

In the acceleration signal $x_{roll}(t)$, the waveforms like $x_{col}(t)$, $x_{slid}(t)$ and a direct current are confused. In the TTFDS, the 1st - 3rd order harmonics $X_{roll}(1)$, $X_{roll}(2)$ and $X_{roll}(3)$ fluctuate with various amplitudes in rolling down. Then, if the influence expressed on the 1st - 3rd order harmonics $X(1)$, $X(2)$, $X(3)$ of frequency distribution appear with various amplitudes continuously over a certain time T_3 , it is considered that the responses are caused by the rolling down of sensing node in landslide. The time T_3 is longer time than the time T_2 . It will be also got by several experiments.

By using the sum of $X(1)$, $X(2)$, $X(3)$ and a threshold level γ , the condition of distinction for the landslide by rolling down of sensing node is defined as follows,

[Condition_3]

$$\begin{aligned}
 & \text{if } \left(\sum_{n=1}^3 X_k(n) > \gamma \right) \\
 & \left\{ \begin{array}{l} \text{if } \left\{ \begin{array}{l} \left(\sum_{n=1}^3 X_{k+2}(n) > \beta \right) \\ \cap \left(\sum_{n=1}^3 X_{k+3}(n) > \beta \right) \\ \vdots \\ \cap \left(\sum_{n=1}^3 X_{k+9}(n) > \beta \right) \end{array} \right\} \\ \cap \left\{ \begin{array}{l} \left(\sum_{n=1}^3 X_{k+2}(n) > \gamma \right) \\ \cup \left(\sum_{n=1}^3 X_{k+3}(n) > \gamma \right) \\ \vdots \\ \cup \left(\sum_{n=1}^3 X_{k+9}(n) > \gamma \right) \end{array} \right\} \\ \end{array} \right\} \\
 & \text{then } \left\{ \begin{array}{l} \text{[the occurrence of landslide]} \\ \end{array} \right\} \\
 & \left. \right\} \text{ where } T_3 = 1 \text{ sec. (10 segments : } k, k+1, \dots, k+9).
 \end{aligned}$$

The time T_3 will be defined by several experiments.

5. CONCLUSIONS

In this paper, the distinction method of landslide disaster by using only the signal of acceleration sensor mounted in the sensing node has been described.

In the time transitions of the 1st - 3rd order harmonics of frequency distribution of the acceleration signal, some characteristics have been found each situation of the sensing node in landslide or at collision with hard blocks. By using the dynamic characteristic of them, we have proposed some

models of the condition for the distinction of landslide. In these models, there are several parameters (three threshold levels α , β , γ and three constant times T_1 , T_2 , T_3). To fix the model, it is necessary that these parameters must be adjusted by several experiments.

The function to distinguish landslide in sensing node enhances the autonomy of sensing network, the efficiency of data communication and the power savement of system. In near future, we will investigate the effectiveness of these models by various kinds of experience at fields.

REFERENCES

- [1] "Information - Communication System of Disasters Prevention", *Sankaido*, pp.1-73, 2003
- [2] Kyoto University Disasters Prevention laboratory, "Foundation Disaster", *Sankaido*, pp.9-21, 2003.
- [3] A.Takei, "Landslide,collapse,mudslide - Prediction and Measure -", *Kashima publishing*, pp.65-77, 1980.
- [4] J. B. Andersen, T. S. Rappaport, and S. Yoshida, "Propagation measurements and models for wireless communications channels," *IEEE Commun. Mag.*, vol. 33, pp. 42-49, 1995.
- [5] Mondinelli, F.; Kovacs-Vajna, Z.M, "Self-localizing sensor network architectures", *IEEE Transactions on Instrumentation and Measurement*, Vol.53, pp.277 - 283, 2004.
- [6] Ferrari, P.; Flammini, A.; Marioli, D.; Sisinni, E.; Taroni, A., "A Bluetooth-based sensor network with Web interface", *IEEE Transactions on Instrumentation and Measurement*, Vol.54, pp. 2359 - 2363, 2005.
- [7] Rahman, F.; Kumar, A.; Nagendra, G.; Gupta, G.S., "Network approach for physiological parameters measurement", *IEEE Transactions on Instrumentation and Measurement*, Vol.54, pp. 337 - 346, 2005.
- [8] Postolache, O.A.; Girao, P.M.B.S.; Pereira, J.M.D.; Ramos, H.M.G., "Self-organizing maps application in a remote water quality monitoring system", *IEEE Transactions on Instrumentation and Measurement*, Vol.54, pp. 322 - 329, 2005.
- [9] Dai-Hua Wang; Wei-Hsin Liao, "Wireless transmission for health monitoring of large structures", *IEEE Transactions on Instrumentation and Measurement*, Vol.55, pp. 972 - 981, 2006.
- [10] Ferrigno, L.; Pietrosanto, A.; Paciello, V., "Low-cost visual sensor node for BlueTooth-based measurement networks", *IEEE Transactions on Instrumentation and Measurement*, Vol.55, pp. 521 - 527, 2006.
- [11] Gao, R.X.; Zhaoyan Fan, "Architectural design of a sensory node controller for optimized energy utilization in sensor networks", *IEEE Transactions on Instrumentation and Measurement*, Vol.55, pp. 415 - 428, 2006.
- [12] Ferrari, P.; Flammini, A.; Marioli, D.; Taroni, A., "IEEE802.11 sensor networking", *IEEE Transactions on Instrumentation and Measurement*, Vol.55, pp. 615 - 619, 2006.
- [13] Flammini, A.; Marioli, D.; Sisinni, E.; Taroni, A., "Environmental Telemonitoring: A Flexible GSM-DECT-Based Solution", *IEEE Transactions on Instrumentation and Measurement*, Vol.56, pp. 1688 - 1693, 2007.
- [14] Lee, K.B.; Reichardt, M.E., "Open standards for homeland security sensor networks", *IEEE Instrumentation and Measurement Magazine*, Vol.8, pp. 14 - 21, 2005.
- [15] Mielke, A.M.; Brennan, S.M.; Smith, M.C.; Torney, D.C.; Maccabe, A.B.; Karlin M JF., "Independent sensor networks", *IEEE Instrumentation and Measurement Magazine*, Vol.8, pp. 33 - 37, 2005.